https://doi.org/10.5194/wes-2022-18
Preprint. Discussion started: 14 March 2022
© Author(s) 2022. CC BY 4.0 License.

eawe european academy of wind energy
Open Access WIND ENERGY SCIENCE DISCUSSIONS

A theoretical framework for the study of power capture enhancement for wind turbines operating at low wind speeds

Irene Miquelez-Madariaga[1], Asier Diaz de Corcuera[2], and Jorge Elso[1]

[1]Public University of Navarre (UPNA), Pamplona, Spain.
[2]Siemens Gamesa Renewable Energy, Sarriguren, Spain.

Correspondence: Irene Miquelez-Madariaga (irene.miquelez@unavarra.es)

Abstract. At below rated operation, wind turbines must track changes in the wind speed to ensure optimal power production. Traditionally, a nonlinear feedback of the generator speed is used for that purpose. In this paper, a linear frequency domain approach to the problem is proposed, that studies the efficiency of the baseline control and the possible benefits of additional strategies. Then, a frequency domain nonlinear relation between wind and energy, that validates the results obtained for the linear model. Lastly, the benefits and costs of an optimal LIDAR based torque signal are discussed.

1 Introduction

As in any other step in the design or operation of a wind turbine, reducing the levelized cost of energy (LCOE) is the main objective in the design of control algorithms. This means that a cost effective operation of a wind turbine requires increasing the annual energy production and extending the lifespan of the machine by reducing loads in the actuators and structural components. Due to the existing trade-off between a maximum energy production and the damage on the machine, two operation zones are defined, that prioritise different objectives.

For high wind speeds, the wind turbine must ensure a constant power production at its rated value. For that purpose, generator torque input is held constant and rotor speed is regulated by pitch the blades.

At below rated operation, the maximum power production point is sought by fixing the pitch angle at its aerodynamic optimum and using the torque to set an adequate generator speed. In this scenario, the generator speed, and thus the generator torque signal, must vary as the wind does.

Indirect Speed Control (ISC, Burton et al. (2001)) is the most well-known strategy for the tracking of the optimum power production point, mostly due to its simplicity -it does not require a complex tuning- and the good results it provides. However, ISC consists on a nonlinear feedback determined by the nonlinear relation between aerodynamic torque, power coefficient (c_P) and generator speed. This fact complicates the analysis of the effect of ISC on the system and the design of new auxiliary strategies to improve the performance of the wind turbine at low wind speeds.

The bibliography identifies three different reasons for a suboptimal behaviour of the wind turbine in terms of power production at below rated operation: yaw misalignment, a poor estimation of the parameters involved in the implementation of the ISC and the slow dynamics of the rotor compared to the change of the maximum power production point. Yaw error appears

https://doi.org/10.5194/wes-2022-18
Preprint. Discussion started: 14 March 2022
© Author(s) 2022. CC BY 4.0 License.

eawe european academy of wind energy
Open Access WIND ENERGY SCIENCE DISCUSSIONS

in turbines with active yaw control strategies, mostly due to the disturbed wind direction measurement provided by nacelle-mounted vanes. LIDAR based strategies for the correction of alignment error such as the described in Zhang and Yang (2020) can operate parallel to ISC and improve the annual energy production up to a 2%.

Systematic losses (Fingersh and Carlin (1998)) are the ones caused by a bad estimation of the parameters involved in the implementation of the ISC. On the one hand, the aerodynamic properties of the wind turbine are not always accurately estimated. More specifically, it is not always easy to identify the optimum of the $c_P - \lambda$ curve due to its flatness. On the other hand, the ISC expression depends on the air density, which can vary due to meteorological changes. Losses up to a 10% are considered in Fingersh and Carlin (1998).

Lastly, tracking losses appear because the rotor speed cannot accommodate the wind changes due to the big inertia of the blades. Studies on the tracking losses are not compelling, as some of them quantify the losses as a 5% of the AEP (Fingersh and Carlin (1998)), whereas others limit them to a 0.4% (Schlipf et al. (2013b)) based on the standard deviation of the tip speed ratio. Besides, the trade-off between energy production and load reduction is considered in Ozdemir et al. (2013), where ISC is discarded as a Pareto-optimal strategy.

Although ISC seems to provide a good performance, adding LIDAR sensors in the control loops allows to explore new strategies based on wind speed measurements (Schlipf et al. (2013b), Ozdemir et al. (2013), Wang et al. (2013)). In order to predict the effect of these new strategies in the performance of the wind turbine, it is necessary to know first what the actual performance of ISC is and what the cost of adding a new control action would be in terms of load increase and actuator damage.

To answer this questions, a theoretical framework for the analysis of the power capture problem in region 2 is carried out. Firstly, the closed loop system has been linearized and represented in the frequency domain. Then, the spectral definition of effective wind speed is compared with the linearized system to predict the effect of the disturbance on the output. In section IV, the possibility of an improvement in power capture is studied. Lastly, the cost of a perfect torque feedforward is given in terms of control action and loads in the axis.

2 Framework for a frequency domain analysis

The problem of the maximization of the energy production at low wind speeds can be tackled from different perspectives. As the rotor speed is one of the most relevant measurable signals within a wind turbine, the search for an optimal power production is often considered a reference tracking problem, where setting an optimal rotor speed reference would require perfect knowledge of the wind.

A much easier interpretation of the problem arises when the power coefficient is used as output. The studied problem then becomes a disturbance rejection one, as the system must remain at the optimal point throughout the changes in wind speed. Consequently, the success of any control strategy can be evaluated based on the frequency distribution of the disturbance (wind) and the controlled system response at the frequencies where the disturbance appears.

https://doi.org/10.5194/wes-2022-18
Preprint. Discussion started: 14 March 2022
© Author(s) 2022. CC BY 4.0 License.

eawe european academy of wind energy
Open Access WIND ENERGY SCIENCE DISCUSSIONS

2.1 Wind turbine model

The present study is carried out for a reduced model of the wind turbine. By only considering the dynamics of the rotor, non idealities such as yaw missalignment are avoided and the torque control for MPPT problem is isolated. More specifically, the wind turbine model used for simulations and calculations is NREL's 5MW wind turbine (Jonkman et al. (2009)), whose most relevant parameters are gathered in Table I. The simplified model (Munteanu et al. (2008)) includes only the dynamics of the rotor described by the equation

$$T_a(t) - i \cdot T_g(t) = J \cdot \dot{\Omega}(t) \tag{1}$$

where i is the gearbox ratio, J is the rotor inertia, T_a is the aerodynamic torque, T_g is the generator torque and $\dot{\Omega}$ is the rotor acceleration.

Likewise, aerodynamic torque is a function of the wind speed $W(t)$ as given by

$$T_a(t) = \frac{1}{2}\rho\pi R^2 c_P(\lambda,\beta)\frac{W^3(t)}{\Omega(t)}. \tag{2}$$

The relation between de power coefficient c_P, the tip speed ratio λ and the pitch angle β is introduced by means of a look-up table obtained from simulations of the complete wind turbine model given by FAST(Jonkman and Buhl Jr (2005)).

Parameter	Symbol	Value
Rotor radius	R	63 m
Rotor inertia	J	25.44 10^6 kg m^{-2}
Gearbox ratio	i	97
Air density	ρ	1.225 kg m^{-3}
Optimal TSR	λ_{OPT}	7.9
Maximum c_P	$c_{P_{MAX}}$	0.4819

Table 1. Parameters of the NREL's 5MW reference wind turbine (Jonkman et al. (2009)).

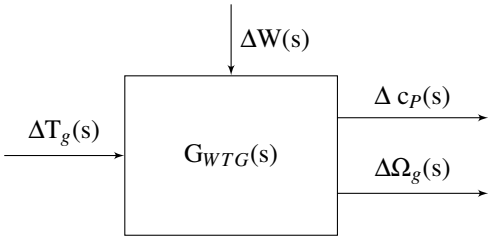

Figure 1. Diagram of the linear open loop system.

The main challenge in the control of wind turbines in region 2 is the dependency of the optimal operation point with the instantaneous wind speed. Usually, accurate measurements or estimations of the wind speed are not available and the control

https://doi.org/10.5194/wes-2022-18
Preprint. Discussion started: 14 March 2022
© Author(s) 2022. CC BY 4.0 License.

eawe european academy of wind energy
Open Access WIND ENERGY SCIENCE DISCUSSIONS

action must be obtained from the feedback of measured variables of the wind turbine. The most widely extended solution for this problem is the Indirect Speed Control (Burton et al. (2001)) strategy, which ensures optimal behaviour in the steady state.

Given that the system is at its steady state and therefore

$$\dot{\Omega}_r(t) = 0, \tag{3}$$

the optimal power production is ensured by guaranteeing a maximum aerodynamic torque and, consequently, a maximum power coefficient. By imposing both conditions in equation 1, the generator torque becomes a function of wind speed as given by

$$T_g(t) = \frac{1}{2}\frac{\rho\pi R^2 c_{P_{MAX}}}{i}\frac{W^3(t)}{\Omega_g(t)}. \tag{4}$$

However, as wind speed is usually unknown or poorly measured, it is estimated by supposing the tip speed ratio is optimal

$$W(t) = \frac{\Omega_g(t)R}{\lambda_{OPT}}. \tag{5}$$

Then, the generator torque becomes

$$T_g(t) = \frac{1}{2}\frac{\rho\pi R^5 c_{P_{MAX}}}{i\lambda_{OPT}^3}\Omega_g^2(t) = K_{OPT}\Omega_g^2(t). \tag{6}$$

The frequency domain analysis of the system requires a linearization of the model. Although wind turbines have two control inputs -pitch angle and generator torque-, at below rated operation the pitch angle is set to the aerodynamic optimum and held constant. Consequently, the power coefficient, which determines the fraction of the available wind energy captured by the wind turbine, depends mainly on two inputs, as shown in Figure 1.

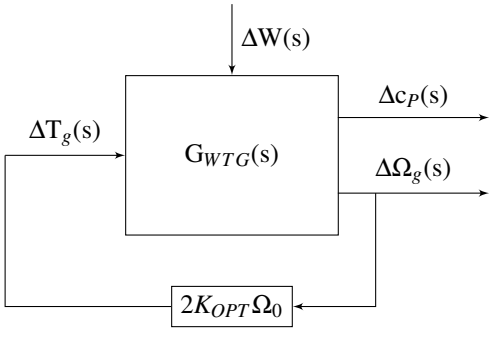

Figure 2. Diagram of the linear closed loop system.

The linear analysis is extended to the Indirect Speed Controller (equation 6) and thus, the relation between generator speed and toque becomes

$$\Delta T_g(t) = 2K_{OPT}\Omega_{0g}\Delta\Omega_g(t) \tag{7}$$

https://doi.org/10.5194/wes-2022-18
Preprint. Discussion started: 14 March 2022
© Author(s) 2022. CC BY 4.0 License.

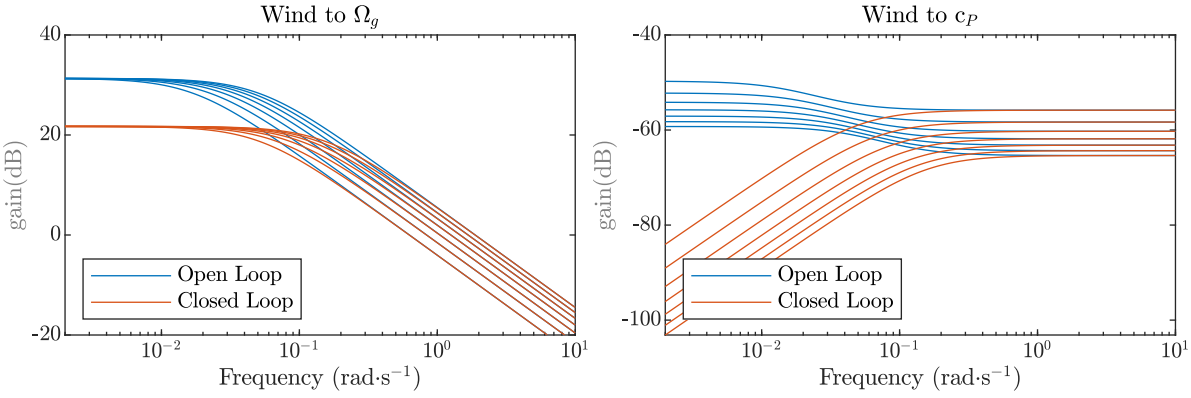

(a) (b)

Figure 3. Representation of the frequency domain of the effect of wind in the generator speed (3a) and the power coefficient (3b). In blue for the open loop and in red for the closed loop system. Each of the lines corresponds to the linearised system at a different operation point determined by wind speed value (3 to 9 m·s^{-1}).

with Ω_{0g} equal to the optimal velocity for a given wind speed. This equation can be included in the block diagram representing the closed loop linear system as shown in figure 2.

Figure 3a shows the Bode diagram between wind speed and generator speed. Both the open loop and the closed loop system can be approximated to a first oder system with different gains in the lower frequencies. The difference between systems becomes more evident when representing the effect of wind in the power coefficient (Figure 3b). Now the open loop system shows no attenuation at the lower frequencies, meaning that a change in the wind speed would make the c_P fall. On the contrary, the controlled system shows good rejection ability of the effect of wind in the power coefficient.

This same behaviour can be observed in the step responses of the open loop and closed systems (Figure 4). Some time after the change in wind speed, the open loop system finds a new steady state at a suboptimal point and the closed loop system goes back to the optimal c_P.

https://doi.org/10.5194/wes-2022-18
Preprint. Discussion started: 14 March 2022
© Author(s) 2022. CC BY 4.0 License.

eawe european academy of wind energy
Open Access WIND ENERGY SCIENCE DISCUSSIONS

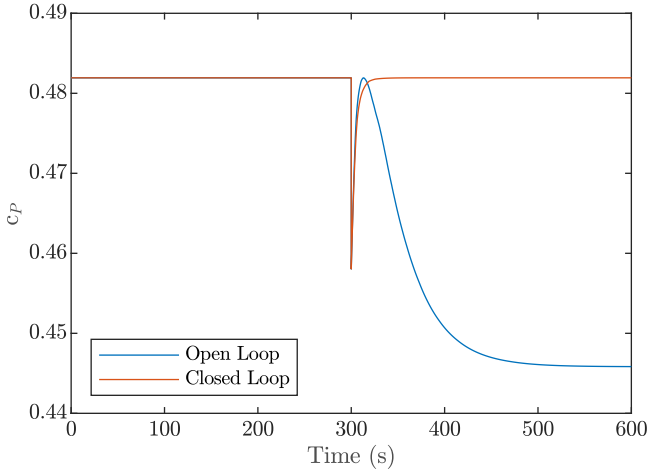

Figure 4. Open loop (blue) and closed loop (red) systems response to a wind step from 5 to 6 m·s^{-1} happening at time 300 s.

2.2 Spectral distribution of wind

To see if the closed-loop system bandwith is enough to reject wind disturbances, the spectrum of the latter must be analyzed. Changes in wind velocity occur at different time scales, from annual variations to high frequency turbulence. Control strategies are mostly determined by turbulent fluctuations, which usually appear at time ranges smaller than ten minutes (Burton et al. (2001)) .

There exist different theoretical models for the spectrum of the longitudinal component of turbulence defined in the frequency domain, which are used in the generation of turbulent wind field data for simulations. One of these models is Kaimal spectrum (Commission et al. (2006)), in which the autospectral density function of the longitudinal component of the turbulence is described as

$$\frac{nS_u(n)}{\sigma_u^2} = \frac{4n\frac{L_{1u}}{W_m}}{\left(1+6n\frac{L_{1u}}{W_m}\right)^{5/3}}, \tag{8}$$

where S_u is the autospectral density function, L_{1u} is a length scale that depends on the dimensions of the wind turbine, n is he frequency in Hz, W_m is the mean wind speed and σ_u^2 is the standard deviation, related to the turbulence intensity.

Kaimal spectrum describes the evolution of wind speed in time at a certain point, for example, at hub height. However, for bigger rotor diameters this information might not be representative of the wind field at the whole rotor plane and thus, does not determine the expected operation of the turbine.

The blades have an averaging effect on the turbulent wind field. Consequently, if a turbulent wind field needs to be simulated in a reduced or linear model, the effective wind would provide a good representation of its effect on the system. Effective wind is defined as the weighted average of the wind at the rotor plane(Wang et al. (2013)) and, for a continuous field, it can be

https://doi.org/10.5194/wes-2022-18
Preprint. Discussion started: 14 March 2022
© Author(s) 2022. CC BY 4.0 License.

eawe european academy of wind energy
Open Access WIND ENERGY SCIENCE DISCUSSIONS

calculated as

$$W_{EFF} = \sqrt[3]{\frac{\int_0^{2\pi}\int_0^R u^3(r,\phi)\frac{\partial c_P}{\partial r} r dr d\phi}{\int_0^{2\pi}\int_0^R \frac{\partial c_P}{\partial r} r dr d\phi}} \tag{9}$$

where $\frac{\partial c_P}{\partial r}$ is the function for the power losses at the tip of the blade, u is the wind speed in the direction perpendicular to the rotor and r and ϕ represent the different points of the rotor in polar coordinates. An equivalent expression for a discrete wind field is

$$W_{EFF} = \frac{\sum_{i=0}^{n} c_{P_i} u_i}{\sum_{i=0}^{n} c_{P_i}} \tag{10}$$

whiere c_{P_i} and u_i are the power coefficient and wind speed at each point of the discrete grid representing the wind field at the rotor plane.

The power spectral density of the effective wind can also be obtained by using the coherence model of the longitudinal velocity component of two points at a certain distance, as explained in Schlipf et al. (2013a). The difference between the spectra of the hub height and the effective wind can be observed in Figure 5, where the higher frequencies of the wind at single points cancel each other out when computing the effective wind speed. As a consequence, the spectrum of the effective wind speed appears at the left of the spectrum of the hub height wind.

3 Power capture and distribution of the power losses

As anticipated in the previous section, the performance of a control strategy can be predicted in terms of the frequency response of the closed loop system and the frequency distribution of the disturbance input. Figure 5 represents this situation perfectly, as it allows to see how the spectrum of the wind speed lies exactly in the frequency range where the controlled system presents a good disturbance rejection. Besides, it also becomes clear why using the hub height wind as input for the simplified model leads to an underestimation of the efficiency of the ISC, as a significant part of its spectrum (0.1 to 0.5 rad·s^{-1}) lies outside of the frequency range with good attenuation.

To extend this analysis into a quantitative result, the first step should consist on stablishing the optimal behaviour. Theoretically, the maximum efficiency for the energy production of a wind turbine is a 59.3% as, given by Betz's law (Burton et al. (2001)). In truth, the efficiency is always slightly lower than Betz's limit and depends on the construction features of each wind turbine. Consequently, for the following analysis, the empirical c_P coefficient is set as the limit for the efficiency. Its value is obtained from the $\lambda - \beta - c_P$ curves obtained from simulation. From the above stated reasons, the maximum available energy in a time series can be expressed as

$$E_{MAX}(t) = \int_0^{t_{end}} \frac{1}{2}\rho c_{P_{MAX}} W_{EFF}^3(t) dt, \tag{11}$$

which would be the energy contained in the effective wind.

https://doi.org/10.5194/wes-2022-18
Preprint. Discussion started: 14 March 2022
© Author(s) 2022. CC BY 4.0 License.

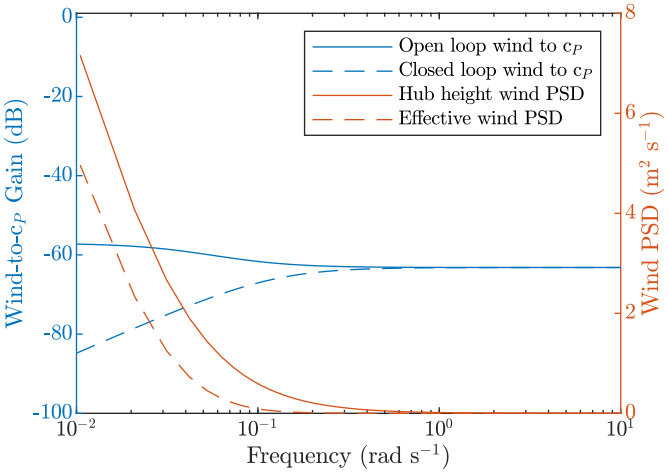

Figure 5. In blue: Bode plot from wind to power coefficient for the open loop (continuous) and closed loop (dashed) system. In red: power spectral density (PSD) of the hub height wind signal (continuous) and rotor effective wind speed (dashed).

On another note, it is of interest to determine which fration of the available energy the wind turbine captures. The captured energy is given by

$$E_{EFF}(t) = \int_0^{t_{end}} \frac{1}{2}\rho c_P(t) W_{EFF}^3(t) dt. \tag{12}$$

The generated energy given by

$$E_g(t) = \int_0^{t_{end}} \Omega_g(t) T_g(t) dt, \tag{13}$$

is not considered in the analysis as it includes the power exchanged with the rotor inertia that depends on the difference between the initial and the final wind speed of each simulation.

In order to get an approximate value of the energy captured by ISC and verify the conclusions obtained from the linear model, simulations for different wind speeds and turbulence intensities have been performed on the reduced system. The results, that represent the ratio between equation 12 and equation 11 (Table II) show that the wind turbine is tracking the maximum power production point almost perfectly.

Although small, energy losses due to the big inertia of the rotor exist. This idea has already been explained by means of the relation between the wind frequency distribution and the Bode diagram of the system. However, the linear approximation only allows a qualitative analysis of the system and does not determine how much of the power is captured or loss at each frequency. For this reason, a nonlinear relation between the wind frequency distribution and its contribution to the total energy in a time series is proposed. The procedure is the following:

- Applying the Discrete Fourier Transform (DFT) to the wind signal, thus obtaining a magnitude ($W(\omega_k)$ and a phase ($\phi(\omega_k)$) spectrum.

https://doi.org/10.5194/wes-2022-18
Preprint. Discussion started: 14 March 2022
© Author(s) 2022. CC BY 4.0 License.

eawe european academy of wind energy
Open Access WIND ENERGY SCIENCE DISCUSSIONS

Wind	TI		
Speed	5 %	10 %	15 %
5 ms^{-1}	99.983 %	99.951 %	99.890 %
7 ms^{-1}	99.983 %	99.953 %	99.889 %
9 ms^{-1}	99.984 %	99.953 %	99.895 %

Table 2. Efficiency of the ISC strategy for different combinations of mean wind speed and turbulence intensity (TI).

– Apply the inverse DFT to synthetize the wind signal from frequencies 0 to k.

$$W_{EFF,k} = \sum_{0}^{k} |W(\omega_k| \cdot sin(2 \cdot \pi \cdot f_k \cdot t + \phi(\omega_k)), \tag{14}$$

– Computing the total energy available in the new wind signal using equation 11.

– Simulating the new wind signal to obtain the captured energy as given by equation 12.

– Assigning the each of the energy values to the frequency k.

https://doi.org/10.5194/wes-2022-18
Preprint. Discussion started: 14 March 2022
© Author(s) 2022. CC BY 4.0 License.

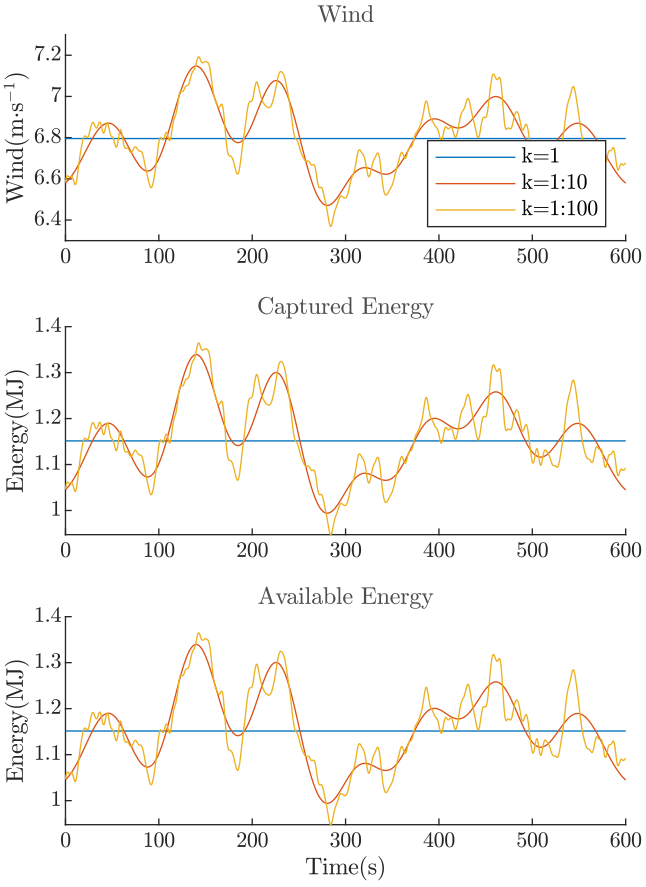

Figure 6. Time series of wind, captured energy and available energy using wind frequencies 1 to k, with k equal to 1 (blue), 10 (red) and 100 (yellow). Adding higher frequencies results in a difference between the available and the captured energy.

The procedure is exemplified in Figure 6. The blue line represents the first component, which corresponds to the constant wind speed. As a consequence, the available and the captured energy are constant too and have the same value, as the system is able to stay in the optimal operation point. The red line appears when the ten first components are added up. The wind is still smooth and both energy signals are quite similar, as the frequence is still in the range in which the disturbance rejection is good. Lastly, the yellow line if formed by the first 100 frequencies and therefore shows some turbulence in it. In this case, the energy signals are not exactly equal. Because the system is not able to track the wind changes perfectly, the captured energy is more rounded in the peaks and valleys.

The results of applying the frequency domain analysis in the whole frequency range are depicted in Figure 7. Firstly, it should be mentioned that adding new frequencies does not guarantee an increase in the total energy as, depending on the phase difference between the different components, the mean wind speed might decrease. Besides, Figure 7 shows how most of the energy is already determined by the mean wind speed, while oscillations only cause small variations of the final value.

https://doi.org/10.5194/wes-2022-18
Preprint. Discussion started: 14 March 2022
© Author(s) 2022. CC BY 4.0 License.

WIND ENERGY SCIENCE DISCUSSIONS

Lastly, the results show the already predicted behaviour. At low frequencies both signals are almost superposed as all energy is captured. From 0.06 rad·s^{-1} on, the signals break apart as power losses start to appear.

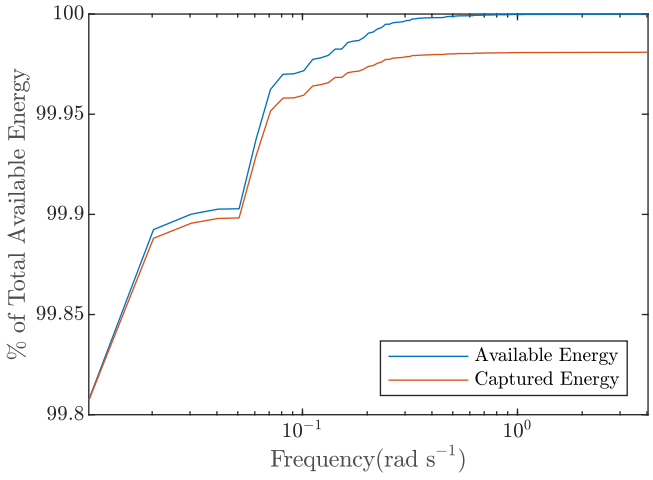

Figure 7. Frequency distribution of the available and captured power of a wind timeseries of mean speed 7 m·s^{-1} and TI=10%.

The main conclusion of this analysis is that we cannot expect a great improvement in the capture energy by adding a supplementary control strategy but they would appear in frequencies between 0.06 and 0.2 rad·s^{-1}, depending on the mean wind speed and the turbulence intensity.

Additionally, the analysis proves the validity of the linearization for explaining the behaviour of the system with the non-linear feedback and for predicting the outcome of the simulations. This means the linear approximation could be used for the development of new strategies to improve in terms of different control objectives such as load reduction.

4 LIDAR based optimal torque feedfoward

Although it has been proven that the ISC performance is very good, it is still of interest to study the cost of an optimal torque feedfoward control.

As shown in Figure 10, the closed loop system has two different inputs, wind ($W(z)$) and feedforward torque signal ($T_{g,FF}(z)$). Consequently it can be model as two transfer functions, the first one represents the effect of wind on the power coefficient and, at an operation point of 7 m·s^{-1} is

$$D_{CL}(z) = k_1 \frac{z+d}{z+p} = -0.0005392 \frac{z-1}{z-0.9969}. \tag{15}$$

The second one represent the effect of the torque signal provided by the feedfoward controller on the output and at the same operation point is

$$P_{CL}(z) = k_2 \frac{1}{z+p} = -6.355 \cdot 10^{-08} \frac{1}{z-9969}. \tag{16}$$

https://doi.org/10.5194/wes-2022-18
Preprint. Discussion started: 14 March 2022
© Author(s) 2022. CC BY 4.0 License.

eawe european academy of wind energy
Open Access WIND ENERGY SCIENCE DISCUSSIONS

The parameters of the two transfer functions vary with the operation point and, therefore, with the wind speed, as shown in Figure 8 .

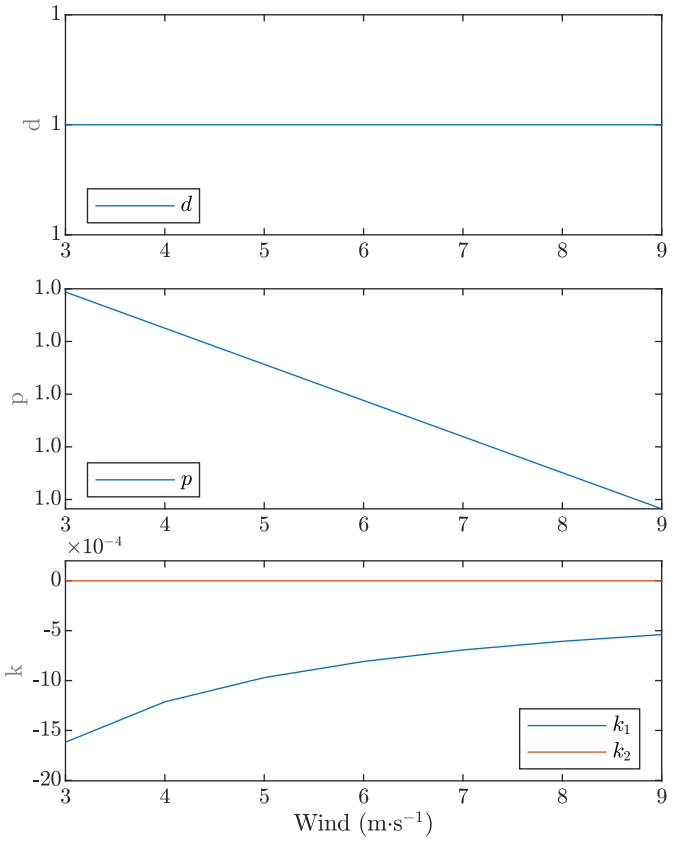

Figure 8. Parameters of the closed loop linear system for different operation points.

The condition imposed on the system to ensure a maximum power production is not to leave the optimal point, determined by the maximum power coefficient, through the wind speed changes. In terms of the transfer functions, this condition is expressed as

$$\Delta c_P(z) = k_1 \frac{z+d}{z+p}\Delta V(z) + \frac{k_2}{z+p}\Delta T_g(z) = 0, \tag{17}$$

which allows to solve for the torque signal as

$$\Delta T_g(z) = -(z+d)\frac{k_1}{k_2}\Delta V(z). \tag{18}$$

As the expresion for the feedfoward controller is based on the parameters of the closed loop system, the feedfoward controller must work along with the ISC. The transfer function between the wind and the torque is non causal, thus requiring information

https://doi.org/10.5194/wes-2022-18
Preprint. Discussion started: 14 March 2022
© Author(s) 2022. CC BY 4.0 License.

eawe european academy of wind energy
Open Access WIND ENERGY SCIENCE DISCUSSIONS

of the wind before it reaches the rotor. They only way to have such information is by using remote sensors that are able to measure wind ahead of the rotor, such as LIDAR sensors. The new structure for the region 2 is represented in Figure 10, where the block F(z) represents the discrete transfer function between wind and torque. The new frequency response can be seen in Figure 9.

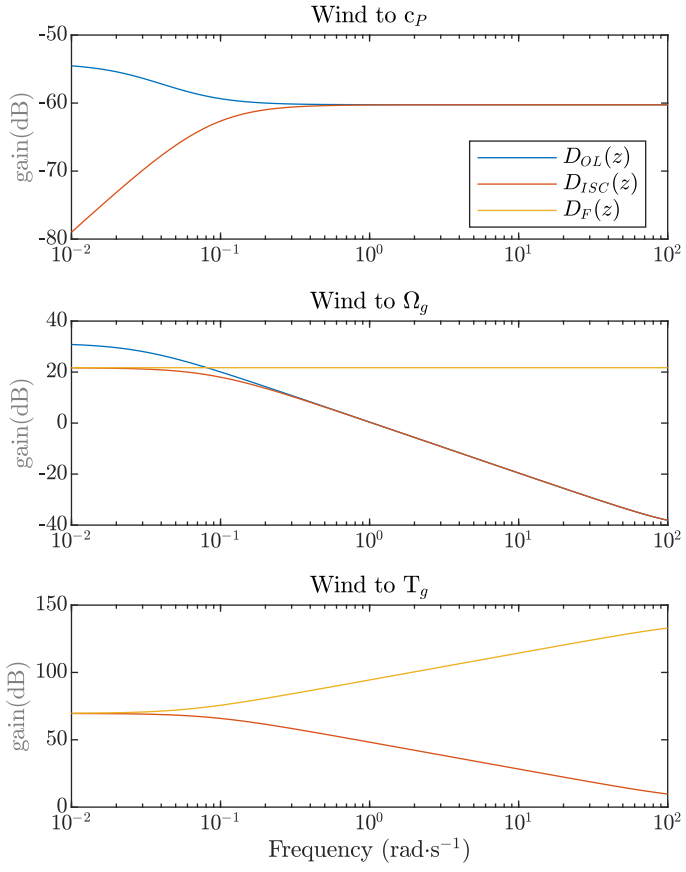

Figure 9. Frequency response of the open loop system (blue), closed loop system (red) and closed loop system with feedfoward (yellow) using wind as an input and power coefficient, generator speed and generator torque as outputs.

https://doi.org/10.5194/wes-2022-18
Preprint. Discussion started: 14 March 2022
© Author(s) 2022. CC BY 4.0 License.

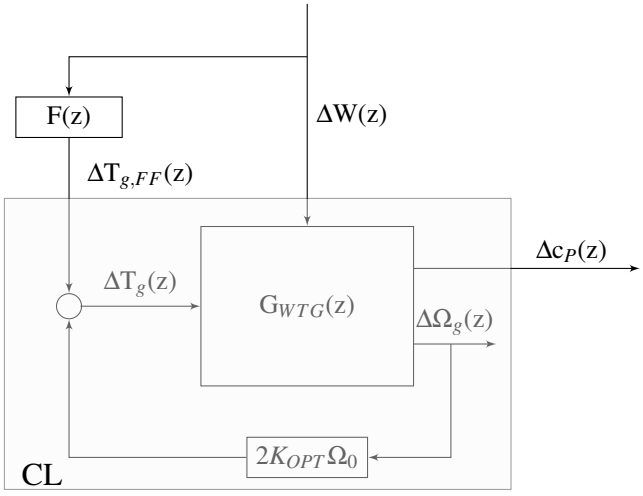

Figure 10. Diagram of the linear open loop system.

Once the feedfoward action is added, the relation between the frequency distribution of the wind and the captured power is obtained as described in section III. Besides, the analysis has been extended to the generator torque, that serves as a good estimator of the longitudinal shaft force. The results are represented in Figure 11 and show how using a perfect wind speed measurement generates negligible improvement in power capture but doubles the standard deviation of the torque signal.

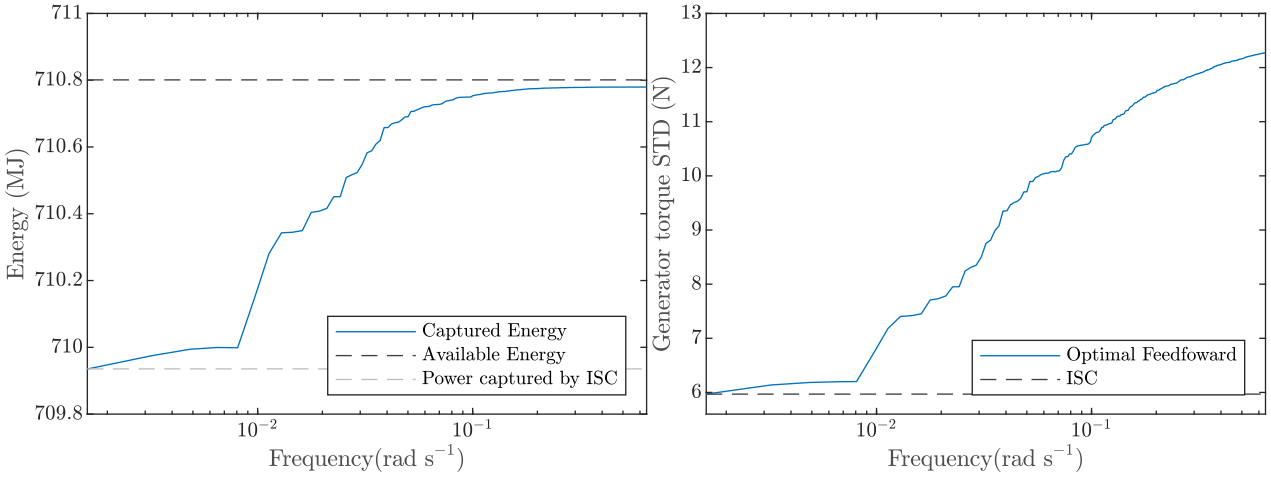

(a) (b)

Figure 11. Representation of the frequency domain of the effect of wind in the generator speed (11a) and the power coefficient (11b). In blue for the open loop and in red for the closed loop system.

https://doi.org/10.5194/wes-2022-18
Preprint. Discussion started: 14 March 2022
© Author(s) 2022. CC BY 4.0 License.

eawe european academy of wind energy
Open Access WIND ENERGY SCIENCE DISCUSSIONS

5 Conclusions

The results on the captured power show that it is not possible to improve the AEP by means of a strategy complementary to ISC. It is therefore advisable to focus on reducing other sources of power losses such as yaw misalignment or a bad estimation of the wind turbine parameters.

However, the linear representation of the open and closed loops systems provide a good representation of the behaviour of the nonlinear complete system. The linearization allows to predict the good performance of the ISC strategy and to design a feedforward controller that generates a torque signal that ensures a perfect maximum power point tracking. This feedforward controller is non-causal. However, this is not necessarily a problem, as LIDAR sensors provide remote measurements of the wind ahead of the rotor. Therefore, they allow using information of the wind before it reaches the rotor.

In practice, this optimal feedforward does not guarantee an improvement with respect to ISC. Firstly, the optimal torque signal appears at higher frequencies, which increases the loads in the shaft. Besides, to ensure optimal tracking, a perfect measurement of the wind is required. Any error introduced by LIDAR sensors will cause a suboptimal behaviour in terms of power capture while increasing the torque action.

Acknowledgements. The authors gratefully appreciate the support given by Siemens Gamesa Renewable Energy through the predoctoral research contract no. 1055/2020.

https://doi.org/10.5194/wes-2022-18
Preprint. Discussion started: 14 March 2022
© Author(s) 2022. CC BY 4.0 License.

References

Burton, T., Sharpe, D., Jenkins, N., and Bossanyi, E.: Wind energy handbook, vol. 2, Wiley Online Library, 2001.

Commission, I. E. et al.: Wind turbines-part 1: design requirements, IEC 614001 Ed. 3, 2006.

Fingersh, L. and Carlin, P.: Results from the NREL variable-speed test bed, in: 1998 ASME Wind Energy Symposium, p. 50, 1998.

Jonkman, J., Butterfield, S., Musial, W., and Scott, G.: Definition of a 5-MW reference wind turbine for offshore system development, Tech. rep., National Renewable Energy Lab.(NREL), Golden, CO (United States), 2009.

Jonkman, J. M. and Buhl Jr, M. L.: Fast user's guide-updated august 2005, Tech. rep., National Renewable Energy Lab.(NREL), Golden, CO (United States), 2005.

Munteanu, I., Bratcu, A. I., Cutululis, N.-A., and Ceanga, E.: Optimal control of wind energy systems: towards a global approach, Springer Science & Business Media, 2008.

Ozdemir, A., Seiler, P., and Balas, G.: Benefits of preview wind information for region 2 wind turbine control, in: 51st AIAA Aerospace Sciences Meeting including the New Horizons Forum and Aerospace Exposition, p. 317, 2013.

Schlipf, D., Cheng, P. W., and Mann, J.: Model of the correlation between lidar systems and wind turbines for lidar-assisted control, Journal of Atmospheric and Oceanic Technology, 30, 2233–2240, 2013a.

Schlipf, D., Fleming, P., Kapp, S., Scholbrock, A., Haizmann, F., Belen, F., Wright, A., and Cheng, P. W.: Direct speed control using lidar and turbine data, in: 2013 American Control Conference, pp. 2208–2213, IEEE, 2013b.

Wang, N., Johnson, K. E., and Wright, A. D.: Comparison of strategies for enhancing energy capture and reducing loads using LIDAR and feedforward control, IEEE Transactions on Control Systems Technology, 21, 1129–1142, 2013.

Zhang, L. and Yang, Q.: A Method for Yaw Error Alignment of Wind Turbine Based on LiDAR, IEEE Access, 8, 25 052–25 059, 2020.